

## Supporting Information

### Photophysical and spectroscopic features of 3,4-dihydro- $\beta$ -carbolines: A combined experimental and theoretical approach

*Fernando Villarruel,<sup>a</sup> M. Paula Denofrio,<sup>a</sup> Rosa Erra-Balsells,<sup>b,c</sup> Ezequiel Wolcan,<sup>d,\*</sup> and Franco M. Cabrerizo<sup>a,\*</sup>*

<sup>a</sup> Instituto Tecnológico de Chascomús (INTECH), Universidad Nacional de San Martín (UNSAM) - Consejo Nacional de Investigaciones Científicas y Técnicas (CONICET), Av. Intendente Marino Km 8.2, CC 164 (B7130IWA), Chascomús, Argentina. E-mail: [fcabrerizo@intech.gov.ar](mailto:fcabrerizo@intech.gov.ar)

<sup>b</sup> Universidad de Buenos Aires. Facultad de Ciencias Exactas y Naturales. Departamento de Química Orgánica. Pabellón II, 3er P., Ciudad Universitaria, (1428) Buenos Aires, Argentina.

<sup>c</sup> CONICET, Universidad de Buenos Aires. Centro de Investigación en Hidratos de Carbono (CIHIDECAR). Facultad de Ciencias Exactas y Naturales. Pabellón II, 3er P., Ciudad Universitaria, (1428) Buenos Aires, Argentina.

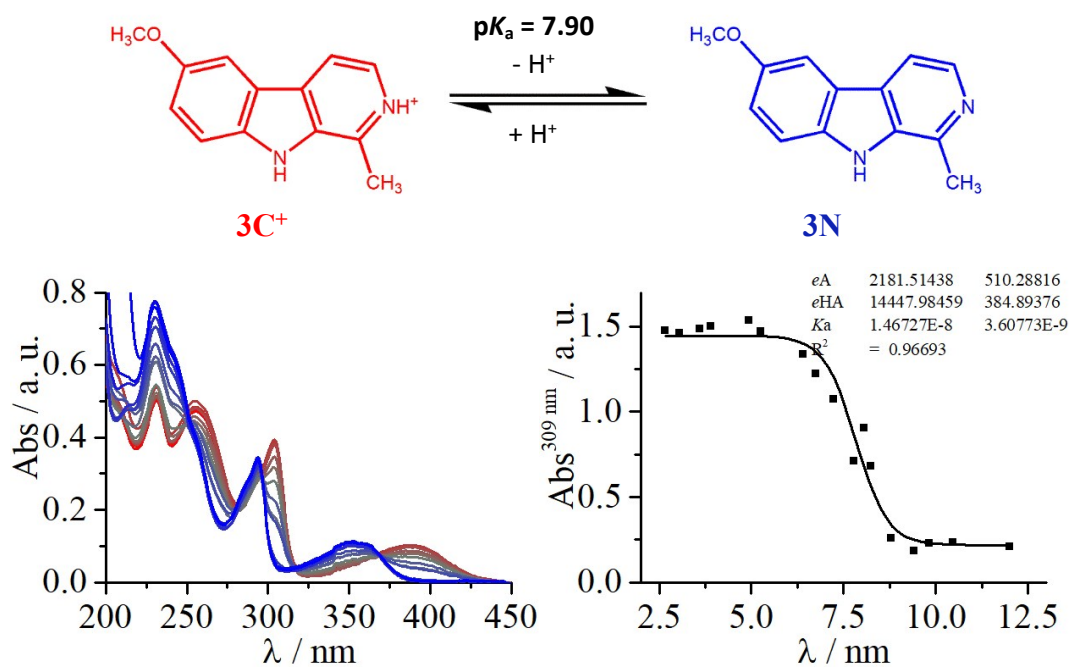
<sup>d</sup> INIFTA - CONICET, Universidad Nacional de La Plata, Diag. 113 y 64 (1900), La Plata, Argentina. E-mail: [ewolcan@inifta.unlp.edu.ar](mailto:ewolcan@inifta.unlp.edu.ar)

\* To whom correspondence should be addressed ([fcabrerizo@intech.gov.ar](mailto:fcabrerizo@intech.gov.ar) and [ewolcan@inifta.unlp.edu.ar](mailto:ewolcan@inifta.unlp.edu.ar))

<b>Contents:</b>	<b><u>Page</u></b>
1. UV-visible spectroscopic titration of <b>3</b> and <b>4</b>	<b>SI.3</b>
2. Mulliken charges of neutral species ( <b>N</b> ) of compounds <b>1</b> to <b>6</b>	<b>SI.4</b>
3. Mulliken charges of <b>7N</b> , <b>7Z(II)</b> , <b>8N</b> , <b>8Z(I)</b> and <b>8Z(II)</b>	<b>SI.5</b>
4. General features of HOMO-1, HOMO and L MOs of <b>1</b> – <b>8</b> .	<b>SI.6</b>
5. Self-Consistent Field energies	<b>SI.9</b>
6. Frontier orbital diagram of anionic species of <b>1</b> to <b>6</b>	<b>SI.10</b>
7. Singlet oxygen phosphorescence signal (at 1270 nm)	<b>SI.11</b>

# 1. UV-visible spectroscopic titration of 3 and 4

(a)



(b)

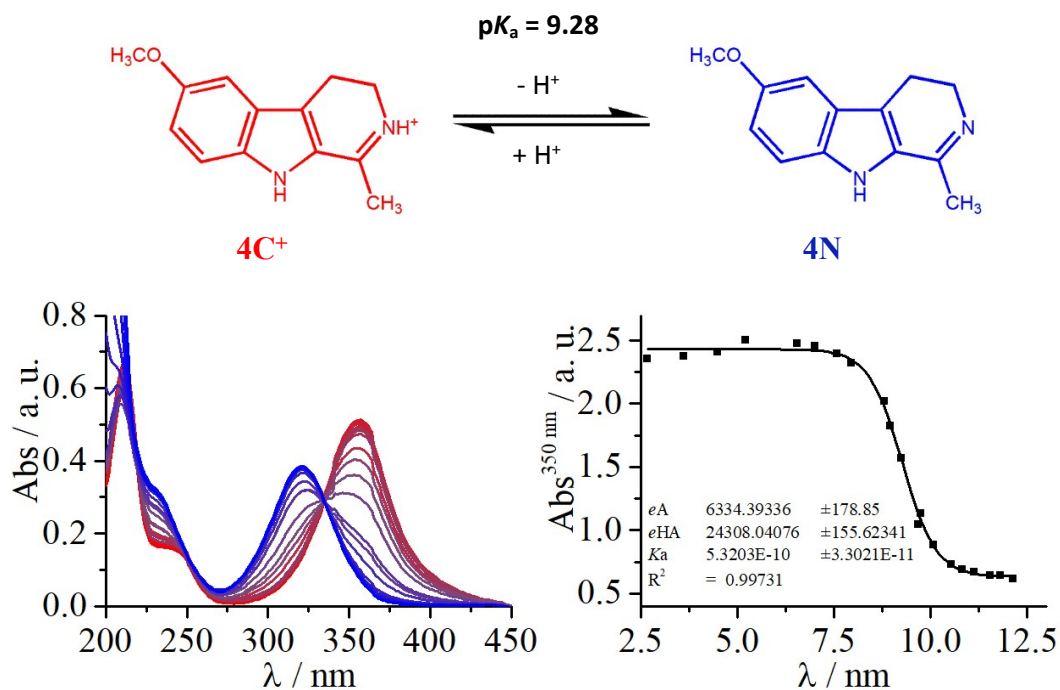


**Figure SI.1.** Acid-base equilibria and UV-visible absorption spectrum pH-evolution and titration curves of (a) 3 and (b) 4.

## 2. Mulliken charges of neutral species (N) of compounds 1 to 6

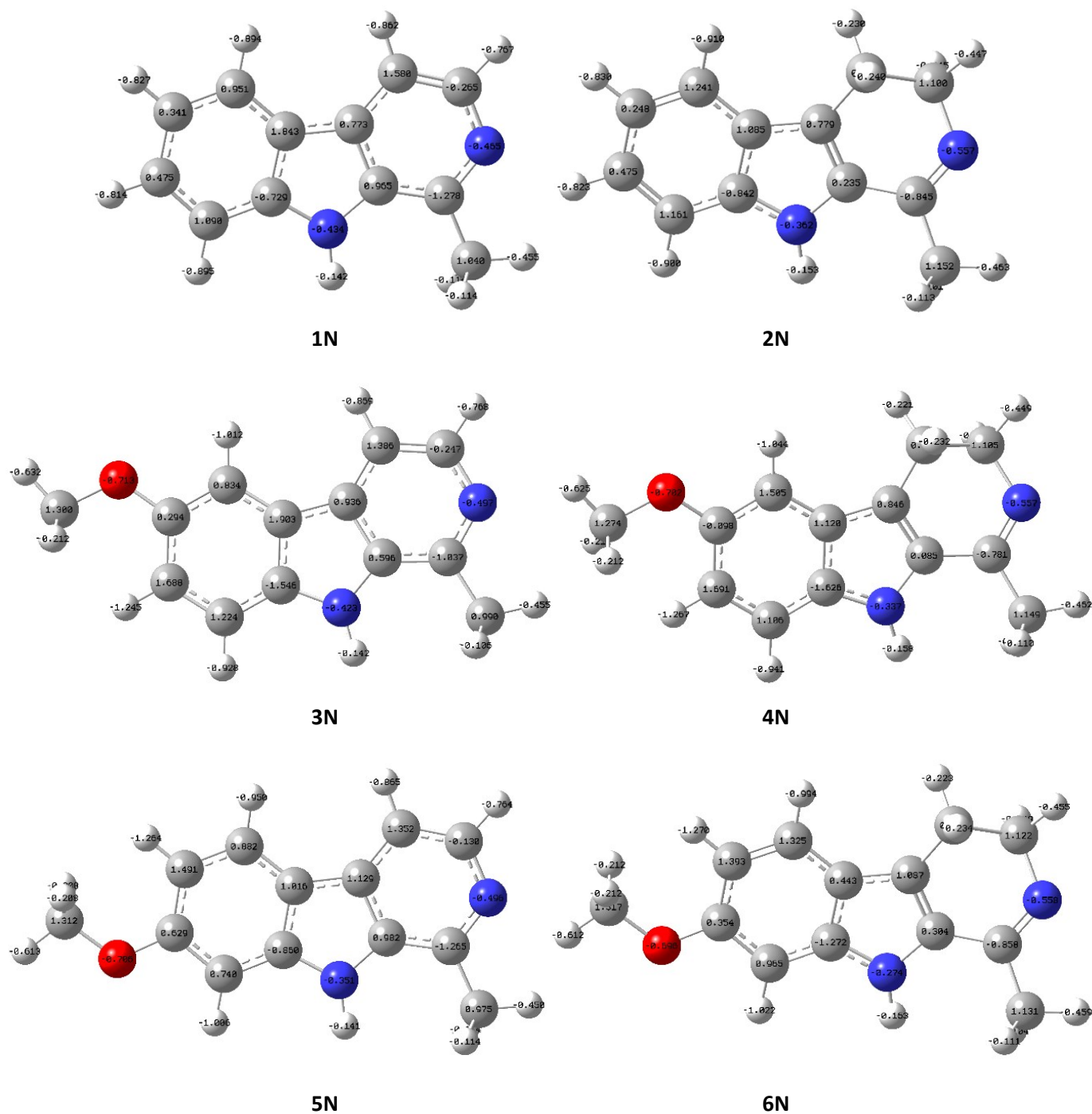


**Figure SI.2.** Chemical formula of 1N, 2N, 3N, 4N, 5N and 6N. In all the cases, the corresponding Mulliken charges are depicted in the center of each atom representation.

### 3. Mulliken charges of 7N, 7Z(II), 8N, 8Z(I) and 8Z(II)

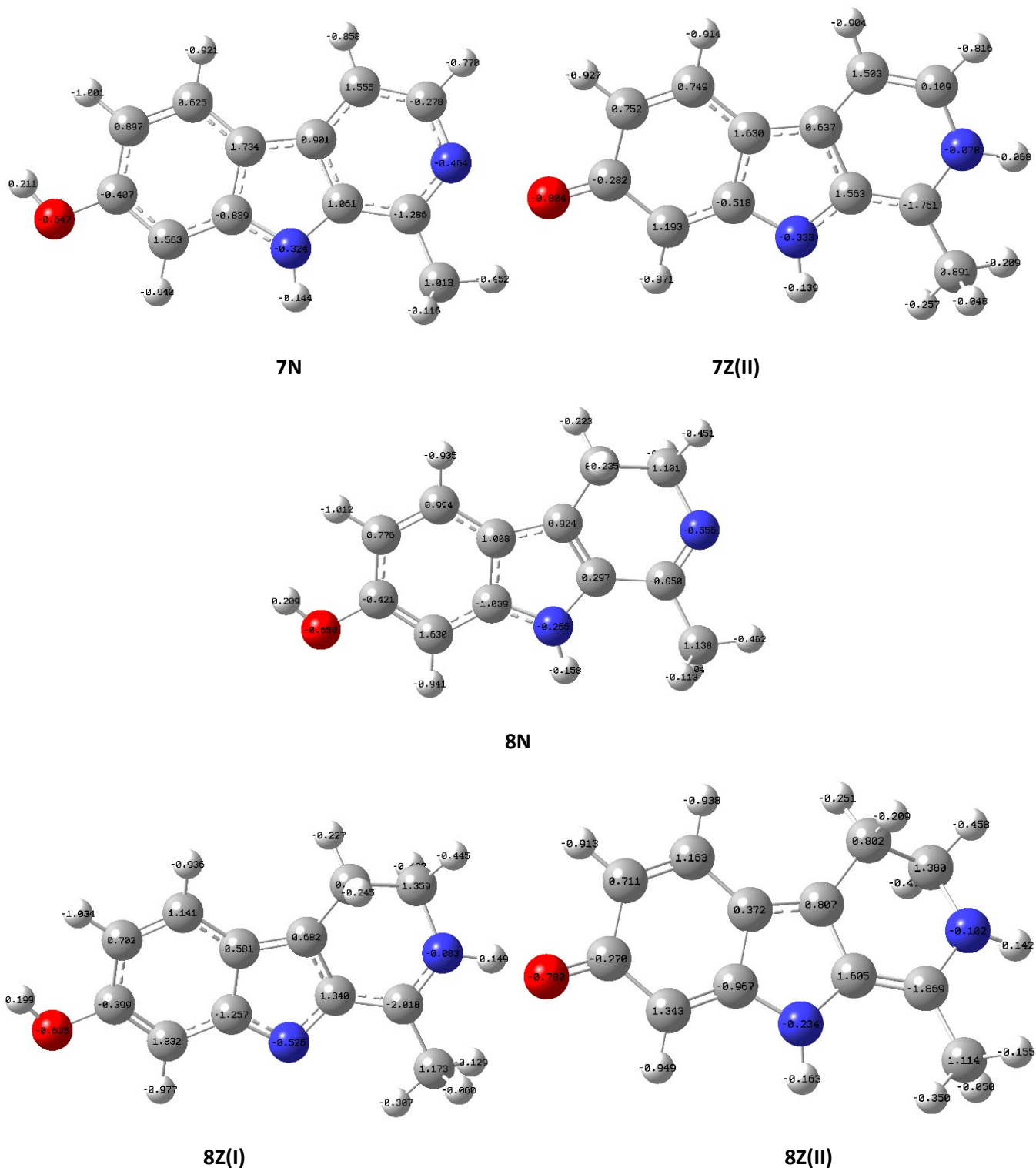


**Figure SI.3.** Chemical formula of neutral and zwitterionic species of **7** and **8**. In all the cases, the corresponding Mulliken charges are depicted in the center of each atom representation.

#### 4. General features of HOMO–1, HOMO and LUMO MOs of 1 – 8.

Based on **Figures 4 - 6** a detailed description of the general features of HOMO–1, HOMO and LUMO MOs is provided herein:

**HOMO and HOMO–1 of 1N, 3N, 5N and 7N.** The HOMO of the neutral species of the four compounds share similar features and thus they will be discussed together. They have a significant amount of electron density connecting C8-C8a-C5a-C4a-C9a-C1 in a distorted bell-shaped form. In addition, there are two bonding regions between C3 and C4 and between C5 and C6 and an isolated significant amount of electron density around N9, with minor contributions of the pyridinic-CH<sub>3</sub> group to the total electron density of H. In **3N**, **5N** and **7N** there are in addition contributions from the O-CH<sub>3</sub> and OH substituent groups. HOMO of **5N** has some significant differences to HOMO of **1N**, **3N** and **7N**. Besides having the same bonding regions C3-C4, C5-C6 and an isolated significant amount of electron density around N9, HOMO in **5N** has electron density between C7-C8 and between C4a-C9a-C1, with no contributions of C5a and C8a to that MO. HOMO–1 of **1N** consist of four lobes of electron density connecting C6-C7-C8; C4-C4a-C9a; C5-C5a-C8a and N2-C3. HOMO–1 of **3N** is very similar to HOMO–1 of **1N** with some additional electron density residing in the O-CH<sub>3</sub> substituent group. HOMO–1 of **5N** consist of four lobes of electron density connecting C6-C7-C8, C5-C5a-C8a, C3-C4-C4a-C9a-N9 and C1-N2 with some additional electron density residing in the O-CH<sub>3</sub> substituent group. HOMO–1 of **7N** is very similar to HOMO–1 of **5N**.

**HOMO and HOMO–1 of 1C, 3C, 5C, 7C, 7Z(I) and 7Z(II).** The spatial features of HOMO in **1C** are almost the same as those of HOMO in **1N**. The spatial features of HOMO–1 in **1C** are very similar to the ones of HOMO–1 in **1N**: four lobes of electron density connecting C6-C7-C8, C4-C4a-C9a-C1, C5-C5a-C8a and N2. Moreover, HOMO and HOMO–1 of **3C** are very similar to HOMO and HOMO–1 of **1C** with the addition of some electron density residing in the O-CH<sub>3</sub> substituent group. HOMO of **5C** is very similar to HOMO–1 of **3C**, the only significant difference being the 6 or 7 positions in the phenyl cycle of the electron density residing in the O-CH<sub>3</sub> substituent group. On the other hand, HOMO–1 of **5C** is nearly identical to HOMO of **3C**, excepting the difference arising from the 6 or 7 positions in the aryl cycle of the electron density residing in the O-CH<sub>3</sub> substituent group. HOMO of **5C** is very similar to HOMO of **7C** as well as HOMO–1 of the former is very similar to HOMO–1 of the latter. HOMO and HOMO-1 of **Z7(I)** are very similar to HOMO and HOMO–1 of **7N**, respectively. HOMO and HOMO–1 of **7Z(II)** are very similar to HOMO and HOMO–1 of **7C**, respectively.

**HOMO and HOMO–1 of 2N, 4N, 6N and 8N.** HOMO of **2N** has a significant amount of electron density in the centers C7-C8, C6-C5-C5a-C8a-N9, C4a-C9a, C1-N2 and C3-C4. HOMO–1 of **2N** has a significant amount of electron density in the centers C5-C6-C7, C8-C8a-C5a-C4a, N9-C9a and C1-N2. HOMO and HOMO–1 of **4N** resemble some similarities with HOMO–1 and HOMO of **2**, respectively. HOMO of **6**

and HOMO of **8** are very similar to HOMO of **2**, the only significant difference being the electron density residing in the O-CH<sub>3</sub> or OH substituent. HOMO-1 of **6N** and HOMO-1 of **8N** are very similar to HOMO-1 of **2N**, the only significant difference being the electron density residing in the O-CH<sub>3</sub> or OH substituent.

**HOMO and HOMO-1 of 2C, 2IC, 4C, 6C, 8C, 8Z(I) and 8Z(II).** The spatial features of HOMO and HOMO-1 in **2C** are very similar to those of HOMO and HOMO-1 in **2N**, respectively. HOMO of **2IC** is very similar to HOMO-1 of **2C**. HOMO-1 of **2IC** has a significant amount of electron density connecting the centers C5a-C5-C6, C7-C8-C8a and C4-C4a. The spatial features of HOMO in **4C** consist of a significant amount of electron density in the centers C5-C6-C7, C8-C8a-C5a-C4a, N9, O-CH<sub>3</sub> substituent, and a very small amount of electron density on C4. The spatial features of HOMO-1 in **4C** consist of a significant amount of electron density in the centers C6-C7-C8, C5-C5a-C8a-N9, C4a-C9a-C1, N2, C3-C4 and O-CH<sub>3</sub> substituent. HOMO of **6C** and HOMO of **8C** are very similar to HOMO of **2C**, the only significant difference being the electron density residing in the O-CH<sub>3</sub> or OH substituent group. HOMO-1 of **6C** and HOMO-1 of **8C** are very similar to HOMO-1 of **2C**, the only significant difference being the electron density residing in the O-CH<sub>3</sub> or OH substituent. HOMO and HOMO-1 of **8Z(I)** and **8Z(II)** are very similar to HOMO and HOMO-1 of **8C**, respectively.

**HOMO and HOMO-1 of 1A to 6A, 7A(II), 8A(I), and 8A(II).** The spatial features of HOMO-1 of **1A**, **3A**, **5A** and **7A(I)** can be described in terms of electron density connecting the centers C6-C7-C8, C5-C5a-C8a-N9, C4-C4a-C9a-C1, N2-C3 and O (for **3A**, **5A** and **7A(I)**). HOMO of **1A**, **3A**, **5A** and **7A(I)** has a significant amount of electron density connecting the centers C3-C4, C5-C6, C7-C8-C8a-C5a-C4a-C9a-C1, N9 and O (for **3A**, **5A** and **7A(I)**). HOMO-1 of **2A**, **4A**, **6A** and **8A(I)** can be described in terms of electron density connecting the centers C5-C6-C7, C4a-C5a-C8a-C8, N9-C9a, N2 and O (for **4A**, **6A** and **8A(I)**). HOMO of **2A**, **4A**, **6A** and **8A(I)** can be described in terms of electron density connecting the centers C5-C6, C7-C8, C8a-N9, C4a-C5a-C9a, C3-C4, N2 and O (**4A**, **6A** and **8A(I)**). HOMO-1 of **7A(II)** has a significant amount of electron density connecting the centers C3-C4, C5-C6, C7-C8-C8a-C5a-C4a-C9a-C1 and N9. HOMO of **7A(II)** has a significant amount of electron density connecting the centers C6-C7-C8, C5-C5a-C8a-N9, C4-C4a-C9a-C1, N2-C3. HOMO-1 of **8A(II)** has a significant amount of electron density connecting the centers C5-C6-C7, C4a-C5a-C8a-C8, C2-C3, N9 and O. HOMO of **8A(II)** has a significant amount of electron density connecting the centers C6-C7-C8, C5-C5a-C8a-N9, C4a-C9a-C1, C3-C4, N2 and O.

**LUMOs.** All the LUMOs for **1N - 8N**, **1C - 8C**, **1A to 6A**, **7A(II)**, **8A(I)**, **8A(II)**, **2IC**, **7Z(II)**, **8Z(I)** and **8Z(II)** compounds are nearly identical. Those LUMOs can be described as an antibonding orbital consisting mainly of electron density over the centers C9a-C1, N2, C3-C4, C4a-C5a, C5, C6-C7 and C8-C8a.

The preceding description of HOMO, HOMO-1 and LUMO for **1N to 8N**, **1C to 8C**, **1A to 6A**, **7A(II)**, **8A(I)**, **8A(II)**, **2IC**, **7Z(II)**, **8Z(I)** and **8Z(II)** compounds is summarized in Tables SI.1 and SI.2.

**Table SI.1:** Compositions of HOMO-1 and HOMO for neutral (N), cationic (C), zwitterionic (Z) and anionic (A) species of **1**, **3**, **5**, **7**. The running number  $i$  on the sum represents each of the different bonded group of atoms contributing with a significant amount of electron density to the particular MO.

Compound	HOMO-1 description	HOMO description
1N	$\Psi_{H-1}^1 = \sum_{i=1}^4 \Psi_{H-1}^1(i)$	$\Psi_H^1 = \sum_{i=1}^4 \Psi_H^1(i)$
3N	$\Psi_{H-1}^3 \cong \Psi_{H-1}^1 + \Psi_{H-1}^{3,C(6)}(O-CH_3)$	$\Psi_H^3 \cong \Psi_H^1 + \Psi_H^{3,C(6)}(O-CH_3)$
5N	$\Psi_{H-1}^5 = \sum_{i=1}^5 \Psi_{H-1}^5(i)$	$\Psi_H^5 = \sum_{i=1}^5 \Psi_H^5(i)$
7N	$\Psi_{H-1}^7 \cong \Psi_{H-1}^5$	$\Psi_H^7 \cong \Psi_H^1 + \Psi_H^{7,C(7)}(O-H)$
7Z(I)	$\Psi_{H-1}^{7Z(I)} \cong \Psi_{H-1}^{7N}$	$\Psi_H^{7Z(I)} \cong \Psi_H^{7N}$
7Z(II)	$\Psi_{H-1}^{7Z(II)} \cong \Psi_{H-1}^{7C}$	$\Psi_H^{7Z(II)} \cong \Psi_H^{7C+}$
1C	$\Psi_{H-1}^{1C} \cong \Psi_{H-1}^1$	$\Psi_H^{1C} \cong \Psi_H^1$
3C	$\Psi_{H-1}^{3C} \cong \Psi_{H-1}^{1C} + \Psi_{H-1}^{3C,C(6)}(O-CH_3)$	$\Psi_H^{3C} \cong \Psi_H^{1C} + \Psi_H^{3C,C(6)}(O-CH_3)$
5C	$\Psi_{H-1}^{5C} \cong \Psi_{H-1}^{1C} + \Psi_{H-1}^{5C,C(7)}(O-CH_3)$	$\Psi_H^{5C} \cong \Psi_{H-1}^{1C} + \Psi_H^{5C,C(7)}(O-CH_3)$
7C	$\Psi_{H-1}^{7C} \cong \Psi_{H-1}^{5C}$	$\Psi_H^{7C} \cong \Psi_H^{5C}$
1A	$\Psi_{H-1}^{1A} = \sum_{i=1}^4 \Psi_{H-1}^{1A}(i)$	$\Psi_H^{1A} = \sum_{i=1}^4 \Psi_H^{1A}(i)$
3A	$\Psi_{H-1}^{3A(I)} = \Psi_{H-1}^{1A} + \Psi_{H-1}^{3A}(O)$	$\Psi_H^{3A} = \Psi_H^{1A} + \Psi_H^{3A}(O)$
5A	$\Psi_{H-1}^{5A(I)} = \Psi_{H-1}^{1A} + \Psi_{H-1}^{5A}(O)$	$\Psi_H^{5A} = \Psi_H^{1A} + \Psi_H^{5A}(O)$
7A(I)	$\Psi_{H-1}^{7A(I)} = \Psi_{H-1}^{1A} + \Psi_{H-1}^{7A}(O)$	$\Psi_H^{7A(I)} = \Psi_H^{1A} + \Psi_H^{7A}(O)$
7A(II)	$\Psi_{H-1}^{7A(II)} = \sum_{i=1}^4 \Psi_{H-1}^{7A(II)}(i)$	$\Psi_H^{7A(II)} = \sum_{i=1}^4 \Psi_H^{7A(II)}(i)$

**Table SI.2:** Compositions of HOMO-1 and HOMO for neutral (N), cationic (C), zwitterionic (Z) and anionic (A<sup>-</sup>) species of **2**, **4**, **6**, **8**. The running number  $i$  on the sum represents each of the different bonded group of atoms contributing with a significant amount of electron density to the particular MO.

Compound	HOMO-1 description	HOMO description
2N	$\Psi_{H-1}^2 = \sum_{i=1}^4 \Psi_{H-1}^2(i)$	$\Psi_H^2 = \sum_{i=1}^5 \Psi_H^2(i)$
4N	$\Psi_{H-1}^4 \sim \Psi_{H-1}^2 + \Psi_{H-1}^{4,C(6)}(O-CH_3)$	$\Psi_H^4 \sim \Psi_H^2 + \Psi_H^{4,C(6)}(O-CH_3)$
6N	$\Psi_{H-1}^6 \sim \Psi_{H-1}^2 + \Psi_{H-1}^{6,C(6)}(O-CH_3)$	$\Psi_H^6 \sim \Psi_H^2 + \Psi_H^{6,C(6)}(O-CH_3)$
8N	$\Psi_{H-1}^8 \cong \Psi_{H-1}^6$	$\Psi_H^8 \cong \Psi_H^6$
8Z(I)	$\Psi_{H-1}^{8Z(I)} \cong \Psi_{H-1}^{8C}$	$\Psi_H^{8Z(I)} \cong \Psi_H^{8C}$
8Z(II)	$\Psi_{H-1}^{8Z(II)} \cong \Psi_{H-1}^{8C}$	$\Psi_H^{8Z(II)} \cong \Psi_H^{8C}$
2C	$\Psi_{H-1}^{2C} \cong \Psi_{H-1}^2$	$\Psi_H^{2C} \cong \Psi_H^2$
2IC	$\Psi_{H-1}^{2IC} = \sum_{i=1}^3 \Psi_{H-1}^{2IC}(i)$	$\Psi_H^{2IC} \cong \Psi_{H-1}^{2C}$
4C	$\Psi_{H-1}^{4C} = \sum_{i=1}^6 \Psi_{H-1}^2(i)$	$\Psi_H^{4C} = \sum_{i=1}^5 \Psi_H^{4C}(i)$
6C	$\Psi_{H-1}^{6C} \cong \Psi_{H-1}^{2C} + \Psi_{H-1}^{6C,C(7)}(O-CH_3)$	$\Psi_H^{6C} \cong \Psi_H^{2C} + \Psi_H^{6C,C(7)}(O-CH_3)$
8C	$\Psi_{H-1}^{8C} \cong \Psi_{H-1}^{2C} + \Psi_{H-1}^{8C,C(7)}(O-H)$	$\Psi_H^{8C} \cong \Psi_H^{2C} + \Psi_H^{8C,C(7)}(O-H)$
2A	$\Psi_{H-1}^{2A} = \sum_{i=1}^4 \Psi_{H-1}^{2A}(i)$	$\Psi_H^{1A} = \sum_{i=1}^4 \Psi_H^{1A}(i)$
4A	$\Psi_{H-1}^{4A} = \Psi_{H-1}^{2A} + \Psi_{H-1}^{4A}(O)$	$\Psi_H^{4A} = \Psi_H^{2A} + \Psi_H^{4A}(O)$
6A	$\Psi_{H-1}^{6A} = \Psi_{H-1}^{2A} + \Psi_{H-1}^{6A}(O)$	$\Psi_H^{6A} = \Psi_H^{2A} + \Psi_H^{6A}(O)$
8A(I)	$\Psi_{H-1}^{8A(I)} = \Psi_{H-1}^{2A} + \Psi_{H-1}^{8A}(O)$	$\Psi_H^{8A(I)} = \Psi_H^{2A} + \Psi_H^{8A}(O)$

<b>8A(II)</b>	$\Psi_{H-1}^{8A(II)} = \sum_{i=1}^6 \Psi_{H-1}^{8A(II)}(i)$	$\Psi_H^{8A(II)} = \sum_{i=1}^6 \Psi_H^{8A(II)}(i)$
---------------	---	---

## 5. Self-Consistent Field energies

**Table SI.3:** Self-Consistent Field (E) energies of different tautomeric species calculated at the B3LYP/aug-cc-pVDZ/PCM(water) level of theory. The difference of energy between C and IC and N and Z is computed for the DH $\beta$ Cs and  $\beta$ Cs, respectively.

DH $\beta$ Cs	E/eV	Tautomer	E/eV	$\Delta E = E(C)-E(IC)$ , eV
<b>2C</b>	-15634.1915	<b>2IC</b>	-15633.4178	-0.773720485
<b>4C</b>	-18750.8849	<b>4IC</b>	-18750.2577	-0.627203232
<b>6C</b>	-18750.9812	<b>6IC</b>	-18750.1759	-0.805274307
<b>8C</b>	-17681.6267	<b>8IC</b>	-17680.8010	-0.82574792
				$\Delta E = E(N)-E(Z)$ , eV
<b>2N</b>	-15621.6174	<b>2Z</b>	-15621.3387	-0.278700057
<b>4N</b>	-18738.3080	<b>4Z</b>	-18738.0215	-0.286499524
<b>6N</b>	-18738.3484	<b>6Z</b>	-18738.0650	-0.283411303
<b>8N</b>	-17668.9929	<b>8Z(I)</b>	-17668.7331	-0.259799127
		<b>8Z(II)</b>	-17668.8795	-0.113425306
<b>8A(III)</b>	-17655.5749	<b>8A(III)</b>	-17655.5749	
<b>8A(II)</b>	-17655.8992	<b>8A(II)</b>	-17655.8992	
<b>8A(I)</b>	-17655.6704	<b>8A(I)</b>	-17655.6704	
$\beta$ Cs	E/eV	Tautomer	E/eV	$\Delta E = E(C)-E(IC)$ , eV
<b>1C</b>	-15601.8235	<b>1IC</b>	-15599.8171	-2.006393422
<b>3C</b>	-18718.5208	<b>3IC</b>	-18716.6794	-1.841402459
<b>5C</b>	-18718.6315	<b>5IC</b>	-18716.5761	-2.055455875
<b>7C</b>	-17649.2668	<b>7IC</b>	-17647.2018	-2.065041499
				$\Delta E = E(N)-E(Z)$ , eV
<b>1N</b>	-15589.4485	<b>1Z</b>	-15589.0408	-0.407702501
<b>3N</b>	-18706.1367	<b>3Z</b>	-18705.7107	-0.426032427
<b>5N</b>	-18706.2132	<b>5Z</b>	-18705.8044	-0.408869734
<b>7N</b>	-17636.8529	<b>7Z(I)</b>	-17636.4624	-0.390483780
		<b>7Z(II)</b>	-17636.5168	-0.336116492
<b>7A(III)</b>	-17623.3580	<b>7A(III)</b>	-17623.3580	
<b>7A(II)</b>	-17623.8542	<b>7A(II)</b>	-17623.8542	
<b>7A(I)</b>	-17623.5930	<b>7A(I)</b>	-17623.5930	

## 6. Frontier orbital diagram of anionic species of 1 to 6.

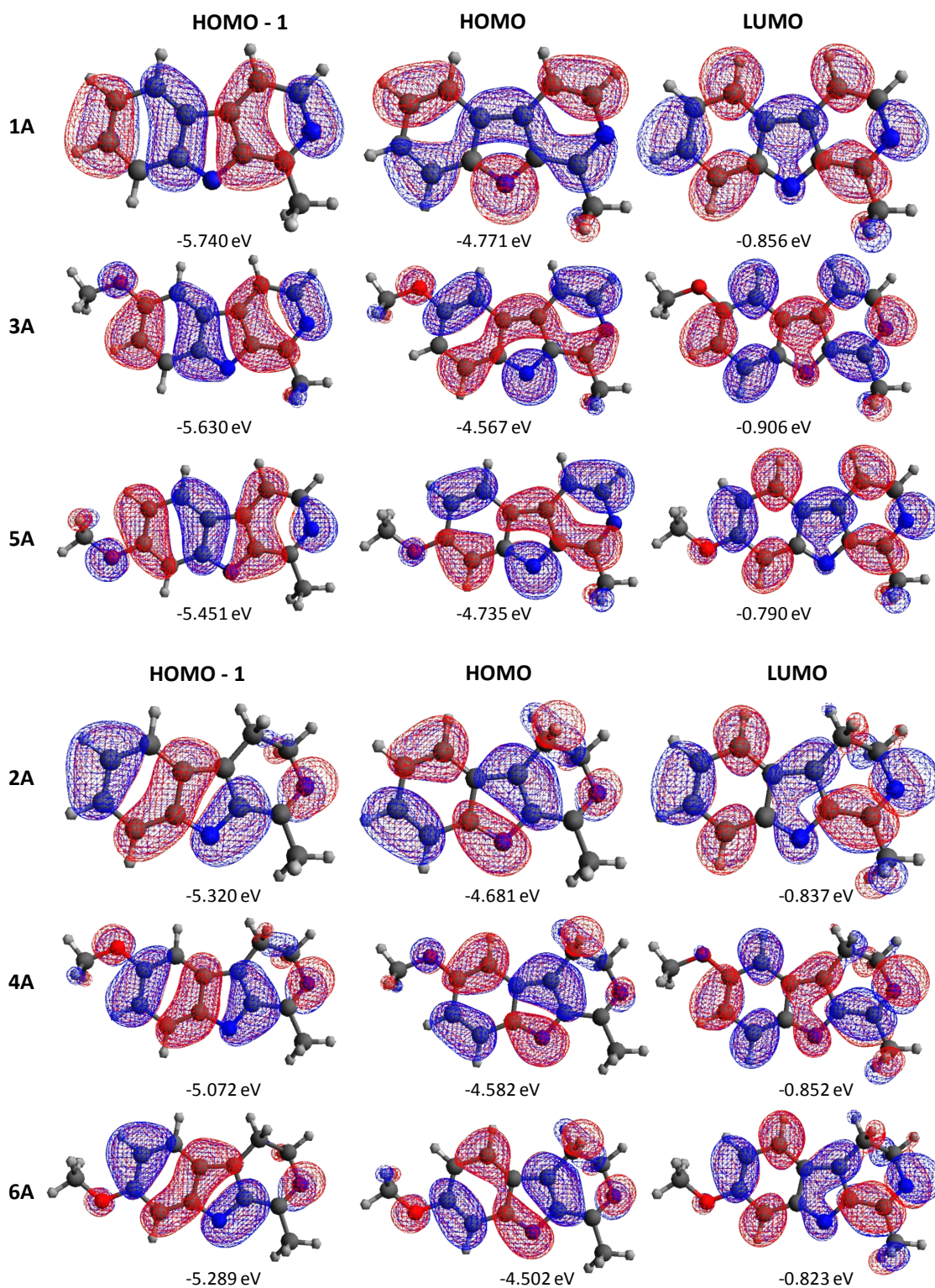


**Figure SI.4.** Molecular orbital diagram of anionic species of compounds **1** to **6** (isocontour value = 0.02). HOMO  $\rightarrow$  LUMO and HOMO-1  $\rightarrow$  LUMO are the main transitions involved in the low energy absorption bands ( $300 \text{ nm} > \lambda > 450 \text{ nm}$ ) of the compounds in  $\text{H}_2\text{O}$ . The vertical transition energies were calculated at the optimized ground-state geometry using TD-DFT calculations (see text for details).

## 7. Singlet oxygen phosphorescence signal (at 1270 nm)

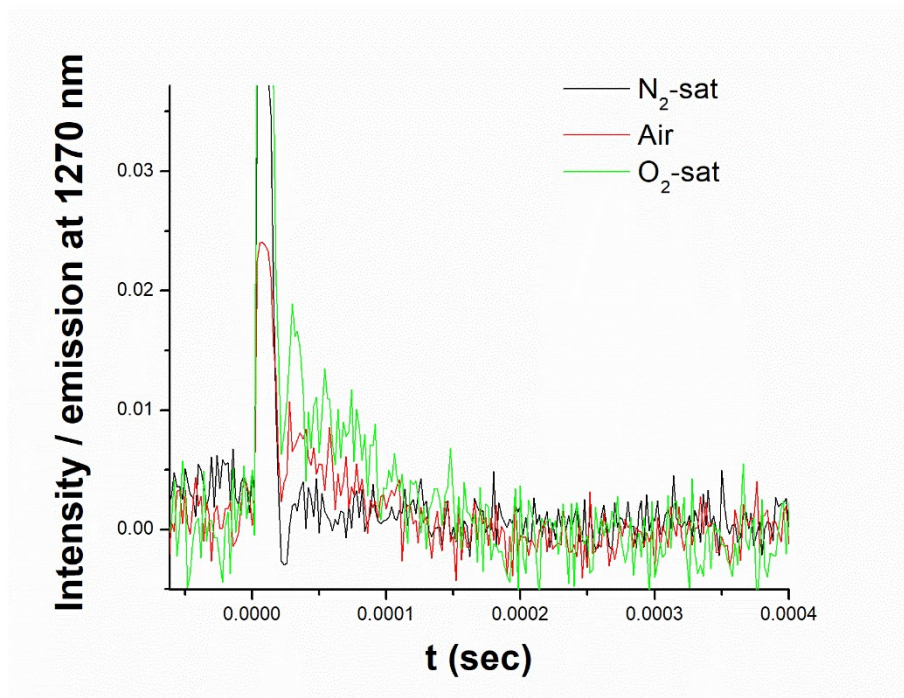


**Figure SI.5.** Representative example of the phosphorescence emission signal recorded from an irradiated sample of compound **3** ( $pD = 7.1$ ) under three different atmospheres ( $N_2$ -sat, air and  $O_2$ -sat).